TU/e EINDHOVEN UNIVERSITY OF TECHNOLOGY

Stability and noise properties of diode lasers with phase-conjugate feedback

Citation for published version (APA):
van der Graaf, W. A., Pesquera, L., & Lenstra, D. (2001). Stability and noise properties of diode lasers with phase-conjugate feedback. *IEEE Journal of Quantum Electronics*, *37*(4), 562-573. https://doi.org/10.1109/3.914406

DOI:
10.1109/3.914406

Document status and date:
Published: 01/01/2001

Document Version:
Publisher's PDF, also known as Version of Record (includes final page, issue and volume numbers)

Please check the document version of this publication:

• A submitted manuscript is the version of the article upon submission and before peer-review. There can be important differences between the submitted version and the official published version of record. People interested in the research are advised to contact the author for the final version of the publication, or visit the DOI to the publisher's website.
• The final author version and the galley proof are versions of the publication after peer review.
• The final published version features the final layout of the paper including the volume, issue and page numbers.

Link to publication

General rights
Copyright and moral rights for the publications made accessible in the public portal are retained by the authors and/or other copyright owners and it is a condition of accessing publications that users recognise and abide by the legal requirements associated with these rights.

• Users may download and print one copy of any publication from the public portal for the purpose of private study or research.
• You may not further distribute the material or use it for any profit-making activity or commercial gain
• You may freely distribute the URL identifying the publication in the public portal.

If the publication is distributed under the terms of Article 25fa of the Dutch Copyright Act, indicated by the "Taverne" license above, please follow below link for the End User Agreement:

www.tue.nl/taverne

Take down policy
If you believe that this document breaches copyright please contact us at:

openaccess@tue.nl

providing details and we will investigate your claim.

Download date: 08. Feb. 2024

Stability and Noise Properties of Diode Lasers with Phase-Conjugate Feedback

Wim A. van der Graaf, Luis Pesquera, and Daan Lenstra, *Member, IEEE*

***Abstract*—For a diode laser subjected to filtered feedback from a phase-conjugating mirror, we present the first exact stability analysis and various noise spectra. The stability properties are intermediate between those of the injection laser and the laser with conventional optical feedback. The role of a finite response-time is to drastically enhance the steady-state stability. For moderate feedback, the frequency noise is suppressed by several orders of magnitude, and the main relaxation frequency of the laser shows a crossover from the usual relaxation oscillation frequency to a new frequency determined by the amount of feedback. This may be of technological importance since it is expected to improve the modulation bandwidth.**

***Index Terms*—Frequency noise, phase-conjugate feedback, relaxation oscillation, semiconductor laser, stability.**

I. Introduction

SEMICONDUCTOR lasers are of considerable importance, for example, in optical communication systems. Their usefulness in coherent optical systems that require low phase noise is hampered by their large linewidth [1] and sensitivity to external optical fields [2], [3], such as (monochromatic) light of an independent source, and feedback from a conventional or phase-conjugating mirror (PCM). This can give rise to many types of instabilities, of which the enhancement of the relaxation oscillation (RO) is the most well known. However, when applied appropriately, optical feedback can also be useful in reducing phase noise.

For stabilization purposes, phase-conjugate feedback (PCF) is preferred over conventional optical feedback (COF), since the laser with COF is very sensitive to mirror distance variations within an optical wavelength [4]. This is due to the fact that with an ordinary mirror, the phase of the returning light depends strongly on the mirror position, while in phase-conjugation with external pumping, this dependence is greatly decreased [5]. Since the linewidth is linked to frequency noise at zero frequency, the linewidth must decrease as well. However, in the case of PCF, one is always confronted with a certain sluggishness of the reflector due to the finite response time, that should be taken into account when analysing the behavior of the laser operation with a PCM. As we will show, this leads to spectral filtering of the laser light. Most of the existing analyses have disregarded this filtering [6]–[8].

Here we present an analysis of the stability and spectral properties of the steady-state single-frequency operation of a single-mode diode laser with PCF, including the finite response time effect in the PCM. The noise spectra are studied in the case of a free-running frequency resonant with the pump. The phase-conjugate signal is assumed to be generated by four-wave mixing in an externally pumped, fast-responding $\chi^{(3)}$-material. For the analysis, we linearize the rate equations around the steady state. The stability is found by evaluating the time evolution of small perturbations from the steady state (disregarding noise), whereas noise spectra are found by investigating how the spontaneous-emission-induced white noise is filtered by the laser. The time-delayed nature of the feedback causes the characteristic equation, the roots of which determine the stability, to have a complicated form. Some approximations have been used in order to solve the characteristic equation [4], [7], [9]. We show, by using another method [10], that in some cases [7], the approximation is not correct. Our results show a new stability region at a moderate feedback rate when a finite mirror response-time is considered. In this stability region, the frequency noise is decreased enormously. This increased stability and noise reduction might lead to an enhancement of the modulation bandwidth of the laser.

II. Rate Equations

When multiple external round trips can be ignored, the rate equations for a single-mode semiconductor laser with sluggish PCF are given by [11]

$$\dot{E}(t) = \frac{1}{2}\left(\frac{\xi\Delta N(t) - \epsilon\Gamma_0 P(t)}{1+\epsilon P(t)} + i\alpha\xi\Delta N(t)\right)E(t) + \frac{\gamma_p}{t_m}e^{2i\delta_0(t-\tau/2)} \times \int_{-\infty}^{t} E^*(\theta-\tau)e^{-(1/t_m+i\delta_0)(t-\theta)}\,d\theta + F_E(t) \quad (1)$$

$$\dot{N}(t) = J - \frac{N(t)}{T_1} - \frac{\Gamma_0 + \xi\Delta N(t)}{1+\epsilon P(t)}P(t) \quad (2)$$

where $N(t) = N_{\rm th} + \Delta N(t)$ is the number of electron–hole pairs (inversion) in the active layer, and where:

$E(t)$ slowly varying amplitude of the optical field with respect to the optical carrier $\exp(i\omega_{\rm th}t)$, with $\omega_{\rm th}$ the

Manuscript received August 1, 2000; revised January 4, 2000. The work of W. A. van der Graaf was supported by the European Community under Project HCM-CHRX-CT94-0592. The work of L. Pesquera was supported by CICYT, Spain, under Project TIC99-0645.

W. A. van der Graaf was with the Instituto de Física de Cantabria (CSIC-UC), Facultad de Ciencias, E-39005 Santander, Spain. He is now with Fortis Bank, Central Risk Management, 1000 AE Amsterdam, The Netherlands (e-mail: wvdgraaf@dds.nl).

L. Pesquera is with the Instituto de Física de Cantabria (CSIC-UC), Facultad de Ciencias, E-39005 Santander, Spain.

D. Lenstra is with the Division of Physics and Astronomy, Faculty of Sciences, Vrije Universiteit, 1081 HV Amsterdam, The Netherlands.

Publisher Item Identifier S 0018-9197(01)02449-6.

0018–9197/01$10.00 © 2001 IEEE

	emission frequency of the solitary laser (i.e., the same laser without feedback) at threshold;
E	normalized such that $\|E(t)\|^2 = P(t)$ equals the number of photons inside the cavity;
$N_{\rm th}$	inversion at threshold of the solitary laser;
ξ	differential gain;
ϵ	nonlinear gain parameter;
Γ_0	photon decay rate;
α	linewidth enhancement factor;
γ_p	feedback rate;
t_m	response time of the mirror;
δ_0	detuning of the mirror pump-beam with respect to $\omega_{\rm th}$;
τ	external cavity round-trip time;
J	number of carriers injected into the active layer per unit of time by means of an electrical current;
T_1	carrier lifetime.

Due to the finite response-time t_m, the feedback term in (1) depends on the optical field at and before time $t-\tau$. In the limit $t_m \to 0$, the feedback term reduces to the one given by, e.g., Van Tartwijk *et al.* [6]. If the mirror responds on a time-scale which is faster than that of all other laser dynamics, instantaneous response is a good approximation. Most research in the literature uses this approximation. However, in practice, the PCM response time will always be finite.

The Langevin forces $F_E(t)$ account for spontaneous emission noise, have an average of zero and are δ-correlated [12]: $\langle F_E(t)\rangle = 0, \langle F_E(t)F_E^*(t')\rangle = R\delta(t-t')$, and $\langle F_E(t)F_E(t')\rangle = 0$, where R is the rate of spontaneous emission into the lasing mode $R = 4\beta N$. Note that the symbol β, which is commonly used in this context, is not the same as the β which is sometimes used as the ratio of spontaneous emission in a mode to the total amount of spontaneous emission.

We proceed by writing down the rate equations in polar coordinates (power and phase instead of the complex electric field). For this, it is handy in further work to first introduce the feedback field $E_{\rm fb}(t)$

$$E_{\rm fb}(t) = \frac{1}{t_m} e^{2i\delta_0(t-\tau/2)} \int_{-\infty}^{t} E^*(\theta-\tau) e^{-(1/t_m + i\delta_0)(t-\theta)}\, d\theta. \tag{3}$$

The single rate-equation (1) is now split into two. Together with an initial condition satisfying (3), these are equivalent to the original (1).

Now we use polar coordinates: $E(t) = \sqrt{P(t)}e^{i\phi(t)}$ and $E_{\rm fb}(t) = \sqrt{P_{\rm fb}(t)}e^{i\phi_{\rm fb}(t)}$ and write down the rate equations for $P, \phi, P_{\rm fb}, \phi_{\rm fb}$ and N

$$\begin{aligned}\dot{P}(t) = {} & \left(\frac{\xi\Delta N(t) - \epsilon\Gamma_0 P(t)}{1+\epsilon P(t)}\right) P(t) \\ & + 2\gamma_p\sqrt{P(t)P_{\rm fb}(t)}\cos[\phi(t)-\phi_{\rm fb}(t)] \\ & + 4\beta N(t) + F_p(t) \end{aligned} \tag{4}$$

$$\begin{aligned}\dot{\phi}(t) = {} & \frac{1}{2}\alpha\xi\Delta N(t) \\ & - \gamma_p\sqrt{\frac{P_{\rm fb}(t)}{P(t)}}\sin[\phi(t)-\phi_{\rm fb}(t)] + F_\phi(t) \end{aligned} \tag{5}$$

$$\begin{aligned}\dot{P}_{\rm fb}(t) = {} & -\frac{2}{t_m}P_{\rm fb}(t) + \frac{2}{t_m}\sqrt{P(t-\tau)P_{\rm fb}(t)} \\ & \times \cos[\phi(t-\tau)+\phi_{\rm fb}(t)-2\delta_0(t-\tau/2)] \end{aligned} \tag{6}$$

$$\begin{aligned}\dot{\phi}_{\rm fb}(t) = {} & \delta_0 - \frac{1}{t_m}\sqrt{\frac{P(t-\tau)}{P_{\rm fb}(t)}} \\ & \times \sin[\phi(t-\tau)+\phi_{\rm fb}(t)-2\delta_0(t-\tau/2)] \end{aligned} \tag{7}$$

$$\begin{aligned}\dot{N}(t) = {} & -2\lambda_R[N(t)-N_{\rm th}] - \{\Gamma_0 + \xi[N(t)-N_{\rm th}]\} \\ & \times \frac{P(t)-P_0-\epsilon P_0 P(t)}{1+\epsilon P(t)}. \end{aligned} \tag{8}$$

We are interested in a state in which the laser emits single-frequency, constant-amplitude light, the steady state. Therefore, we disregard the Langevin noise terms, but take into account the average noise-effect as expressed by the term $4\beta N(t)$ in (4). In the steady state one, has $P(t) = P_{\rm fb}(t) = P_s, N(t) = N_s$, and $\phi(t)$ and $\phi_{\rm fb}(t)$ are varying linearly with time. This can happen only when the laser is locked to the frequency δ_0 of the mirror pump-beams. It then follows that $\phi(t) = \delta_0 t + \phi_s$ and $\phi_{\rm fb}(t) = \delta_0 t - \phi_s$.

Without noise and nonlinear gain ($\beta = 0$ and $\epsilon = 0$) the solutions, if they exist, are found to be

$$N_s = N_{\rm th} + \frac{2\alpha\delta_0 \pm 2\sqrt{\gamma_p^2(1+\alpha^2)-\delta_0^2}}{\xi(1+\alpha^2)} \tag{9}$$

and

$$P_s = P_0 - \frac{2\lambda_R(N_s - N_{\rm th})}{\Gamma_0 + \xi(N_s - N_{\rm th})} \tag{10}$$

where P_0 is the intensity of the solitary laser. After solving for the power and inversion, the phase ϕ_s can be found as well. This phase is determined by the interaction of the laser and the PCM (pump). In fact, it is the phase difference between the laser light and that of the pump. It can only be varied via other parameters, such as the detuning frequency. Therefore, we disregard it in the remainder of this paper. From (9), one can see that steady state is obtained if, and only if, the frequency δ_0 satisfies

$$|\delta_0| \le \gamma_p\sqrt{1+\alpha^2}. \tag{11}$$

This defines a locking range, in close analogy with the injection laser.

For a laser *with* nonlinear gain, and taking into account the average effect of noise, the situation is more complicated, and we treat the noise and nonlinear-gain effects as perturbations and iterate numerically. As a starting guess, we take the steady state without nonlinear gain whenever possible. Otherwise, i.e., outside the locking range, we start from the solitary laser steady-state. Since nonlinear gain describes the intensity-induced change of the laser dynamics, the intensity of the initial guess is used for calculating a modified inversion. This inversion is then used for determining a new value for the laser light intensity. This procedure is repeated a few times until the desired accuracy is obtained.

In the case of a diode laser with conventional optical feedback, the external round-trip delay gives rise to "external cavity modes" (ECMs). This is related to the corresponding round-trip

phase $\Delta\omega\tau$ being equal to a an integral multiple of 2π. The number of ECMs involved is then roughly equal to

$$\gamma\tau\sqrt{1+\alpha^2}$$

(see [2]). Hence, even for moderate amounts of feedback, there may be already a lot of ECMs, where each ECM corresponds to a steady state of monochromatic laser operation. In the present case of phase-conjugate feedback, buildup of round-trip phase is also possible, but locking to a nonzero integral multiple of 2π is impossible, as follows from the steady state analysis described above. Indeed, the only possible steady state corresponds to locking of the laser to the pump frequency of PCM, in which case the round-trip phase vanishes exactly.

III. Stability of the Steady State

Considering small deviations from the steady state allows one to derive the local stability of the steady state and the laser spectra. The stability is found by studying the growth or decay of the deviations, while the noise spectra are found by looking into how the spontaneous emission noise propagates in the laser light fluctuations. The usual way to investigate this is to consider the rate equations when linearized around the steady state. Concerning the stability, the information thus obtained is the local stability. In other words, if the fixed point turns out to be stable, there may still be other attractors, which may even have a larger basin of attraction. The spectra which are calculated using linearized rate equations are accurate only when the noise fluctuations are not so large that nonlinearities must be taken into account.

Defining the vector $\mathbf{x}(t)$ as the deviation from the steady state, $\mathbf{x}(t) = (P(t) - P_s, \phi(t) - \delta_0 t - \phi_s, N(t) - N_s, P_{\mathrm{fb}}(t) - P_s, -\phi_{\mathrm{fb}}(t) + \delta_0 t - \phi_s)$, we find the linearized rate-equations, which form a system of five coupled linear delay-differential equations, with the additional Langevin noise:

$$\dot{\mathbf{x}}(t) = A\mathbf{x}(t) + A'\mathbf{x}(t-\tau) + \mathbf{F}(t). \tag{12}$$

We now calculate the stability and, therefore, disregard the Langevin noise. The system can be formally solved using Laplace-transform techniques [13]. Laplace transformation yields

$$(sI - A - e^{-s\tau}A')\tilde{\mathbf{x}}(s) = \mathbf{x}(0) \tag{13}$$

where I is the unit matrix.

The laser system, as described by (9), is locally stable if, and only if, all roots of the characteristic equation $D(s) = \det(sI - A - e^{-s\tau}A') = 0$ are located in the negative half-plane, that is, to the left of the imaginary axis. Our search for the stability of the laser with phase-conjugate feedback is thus equivalent to knowing whether or not all roots of the corresponding characteristic equation have negative real parts. Writing out the full s-dependence of $D(s)$ yields

$$\begin{aligned} D(s) = {} & s^5 + d_4 s^4 + d_3 s^3 + [d_{20} + d_{21}\exp(-s\tau)]s^2 \\ & + [d_{10} + d_{11}\exp(-s\tau) + d_{12}\exp(-2s\tau)]s \\ & + [d_{00} + d_{01}\exp(-s\tau) + d_{02}\exp(-2s\tau)] \end{aligned} \tag{14}$$

TABLE I
Values of the Parameters Used in the Calculations

Parameter description	Quantity	Value	Unit
Inverse photon lifetime	Γ_0	7.2595×10^{11}	s^{-1}
Injection current	J	4.0635×10^{17}	s^{-1}
Threshold inversion	N_{th}	7.74×10^{8}	-
Carrier lifetime	T_1	2.0×10^{-9}	s
Linewidth enhancement factor	α	3.0	-
Linear gain coefficient	ξ	1.19×10^{3}	s^{-1}
Nonlinear gain coefficient	ϵ	3.57×10^{-8}	-

where the coefficients d_i are functions of the laser parameters and the steady state under consideration. In the case of instantaneous feedback, a third order polynomial is obtained, where again some of the coefficients contain an exponential term. Explicit expressions for the coefficients d_i can be found in [3] or the Appendix. Here, we clearly see why it is more difficult to determine the stability of a feedback system than that of a system without time delay ($\tau = 0$): without delay, $D(s)$ would be a polynomial in s, which can easily be solved. The presence of the exponential $e^{-s\tau}$ makes analytical progress difficult, since in general $D(s) = 0$ has infinitely many roots which cannot be found analytically. Therefore, we will resort to another method to solve for the stability; that is, we do not calculate the roots explicitly.

There is a simple case, however, where one can determine the stability immediately: if $D(0)$ is negative, there must be at least one positive real root, and hence the system is unstable. Without noise, and assuming linear gain, the criterion $D(0) > 0$ is equivalent to the requirement that $\cos(2\phi_s + \arctan\alpha) > 0$. Consequently, of the two solutions in (9), the one with the largest inversion is always unstable. This does not imply stability for the other solution.

Because, in general, one cannot determine the stability easily, the exponential is sometimes approximated in the literature by expanding it to first order: $e^{-s\tau} \approx 1 - s\tau$. In many cases, this is a poor approximation: when the RO undamps, one has $s = i\Omega$, where for low feedback-rates Ω will be close to the angular RO frequency of the solitary laser $\omega_R = \sqrt{\Gamma_0\xi P_0}$. Taking a realistic value of the RO of 3 GHz, $\Omega\tau$ already equals one for a cavity length of less than a centimeter. Without trying to be exhaustive, other approaches found in the literature are: assuming certain parameters to be small [9], or a numerical search for the roots [14].We use an alternative approach by using the principle of the argument in an exact determination of the fixed-point stability (see the Appendix).

A. Results

The technique outlined above is now used for calculating stability diagrams, where we use parameter values as listed in Table I. These values, which are identical to those used by DeTienne *et al.* [11], correspond to a laser pumped 5% above its solitary threshold, and $\omega_R/2\pi = 764$ MHz. Variation of α and ϵ confirms the well-known behavior; that is, a larger α gives rise

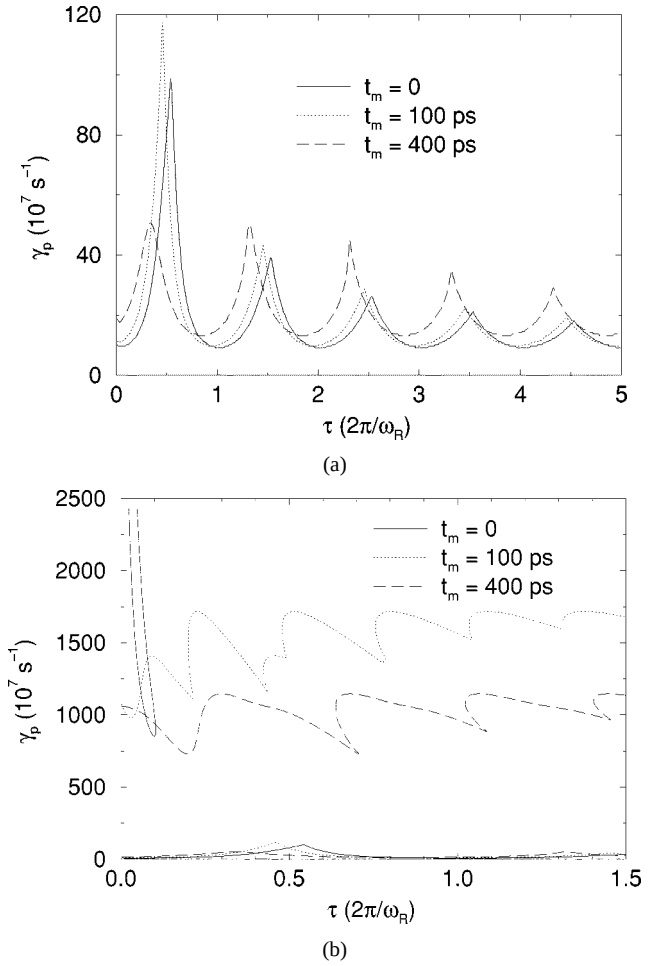

Fig. 1. Feedback rate γ_p at which the laser changes stability as a function of the cavity round-trip time τ, normalized to the RO period. (a) The laser is stable for low feedback and becomes unstable upon increasing γ_p. The stability boundary depends periodically on τ. (b) Increasing the feedback rate further , the laser becomes stable again, due to the sluggishness of the mirror.

to a smaller region of stability, whereas the inclusion of nonlinear gain enhances the stability. In the graphs presented here, the gain is taken to be linear.

For the case of zero detuning ($\delta_0 = 0$), Fig. 1 shows the stability diagram when γ_p and τ are varied for several values of the mirror response time. Focusing first on $t_m = 0$ only, we see that for very small feedback rates, the laser is stable [see Fig. 1(a)]. Upon increasing the feedback, it becomes unstable. Note the periodic modulation of the stability-edge curve with a lower stability-limit when the RO matches an external round-trip resonance; that is, when $\omega_R\tau/2\pi$ is an integer. This was not seen by Agrawal and Gray [7] due to the above-mentioned lowest order expansion of the exponential. On the other hand, it is similar to what was found by Ritter and Haug [9] and Mørk [15] for a laser with COF, although they found higher stability tongues at *integral* values of $\omega_R\tau/2\pi$. This behavior for the PCF from an instantaneous mirror has also been discussed by Murakami and Ohtsubo [16]. As yet, we have not found an explanation for this apparent difference.

Comparing PCF from an instantaneous mirror with that from a slow mirror, we see that the stability enhances slightly with increasing t_m. This is caused by the mirror-induced spectral filtering of the reflected field, suppressing frequencies larger than $1/t_m$. A similar behavior was found recently in the case of COF [17]. More striking is the shifted location of the stability peaks which, in view of the time delay in the mirror, resembles a situation of an external round-trip length larger than in an instantaneous mirror. The effective round-trip length enhancement is not sharply defined, which reduces the quality of the resonance for large t_m. Since the relative importance of this increases when τ gets smaller, this may explain why the peak at $\omega_R\tau/2\pi = 0.5$ is lower for t_m =400 ps than for shorter response times.

We also investigate the behavior at moderate feedback. The result is plotted in Fig. 1(b) [note the different scales along both the X–Y-axes, compared to Fig. 1(a)]. The stability of the laser is enhanced enormously by the sluggish mirror: for an instantaneous mirror there is only a small region for short cavities where stability is found at higher values of the feedback rate, whereas over the whole range of τ indicated in the figure, the PCF laser is stable at higher feedback for mirror response times of 100 and 400 ps. DeTienne *et al.* [11] already found in numerical simulations that the standard deviation of the output power was much smaller for reflectivities on the order of 4%. Here, we have shown that it corresponds to stable steady-state operation of the laser. In the instability region, DeTienne found pulsations of which the frequency increases with γ_p. In Section IV-A, we will consider this resonance frequency in more detail and derive an expression for it. The structure in the higher stability boundaries of the right figure is caused by this frequency matching an external round-trip resonance. Therefore, this is analogous to the oscillations in Fig. 1(a).

The influence of the detuning δ_0 on the stability is shown in Fig. 2. For weak feedback we see a narrow band of stable operation, but this band widens for higher feedback and, finally, we find a large region of stable laser output, which is consistent with Fig. 1(b). Notice that for an instantaneous mirror one has not reported such large regions of stability. The general shapes of the curves for finite t_m resemble the stability diagram of a diode laser with external optical injection [18]. Also, the low-feedback part of the stability diagram with $\omega_R\tau = 1$ is very similar to the corresponding part of the injection laser stability diagram. Again, we see here the destabilizing influence of the RO matching an external round-trip resonance [see Fig.2(b)].

As a last result, we show the effect of a higher pump current on the stability diagrams in the (τ, γ_p)-plane for zero detuning. Fig. 3 has the same parameters as Fig. 1, except that the current is now 50% above threshold, instead of 5%. There are two major changes: due to the higher RO frequency, there are more oscillations in the same range of τ, and the stability at moderate feedback sets in at a higher feedback strength. When we calculate spectra in the next section, we take the laser to be pumped 50% above threshold.

All stability diagrams were checked by direct numerical integration of rate equations (1) and (2) at several points of the stability diagrams, and no discrepancy between the two methods was found.

In line with our results, Bochove [14] reports on stable behavior regardless of the feedback strength for certain values of the "phase" in a laser with an instantaneous mirror. This could correspond to the channel of stable laser operation, as shown in

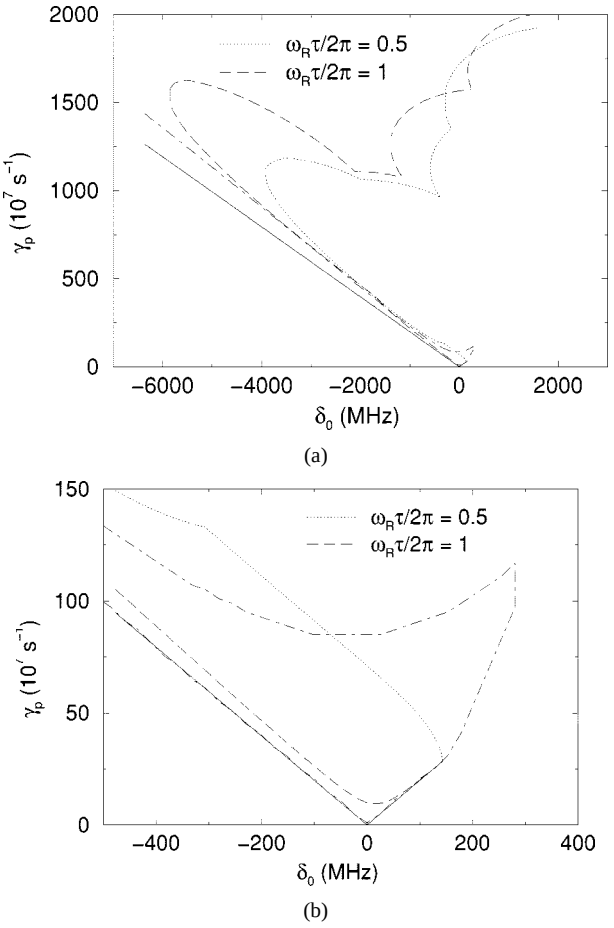

Fig. 2. Stability of the PCF laser as a function of γ_p and the pump detuning δ_0. The dashed-dotted curve corresponds to an instantaneous mirror at $\omega_R\tau/2\pi = 0.5$. All other curves have; $t_m = 100$ ps. To the left of the solid line, no steady-state solutions exust, independent of τ or t_m; therefore, the solid line indicates the locking range. (b) A close-up of the region near the origin of (a).

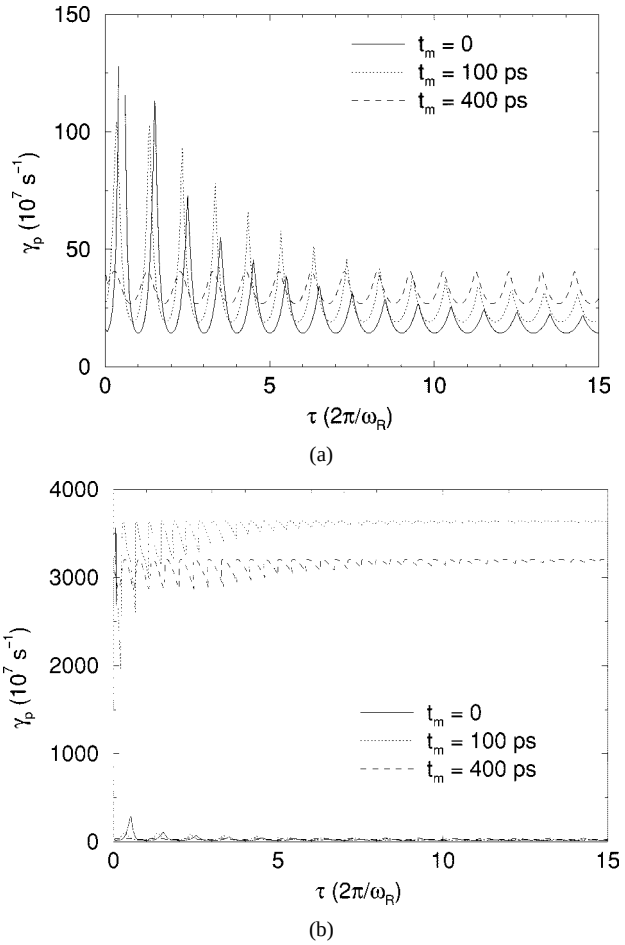

Fig. 3. Stability diagram of a PCF laser pumped 50% above threshold for: (a) low and (b) moderate feedback rates. Due to the higher RO frequency, $\omega_R\tau$ oscillates more rapidly with τ than in Fig. 1.

Fig. 2. However, due to the different representation, his results are sometimes difficult to compare with ours. Note that our main concern here is the influence of the response time of the mirror, which Bochove addresses very briefly. He has not performed a systematic analysis of t_m and, for example, did not find the upper stability regime as depicted in our Fig. 1(b).

Experimental work on phase-conjugate feedback in a diode laser was reported by Andersen *et al.* [19]. In this experiment, an externally pumped rubidium cell was used as a phase-conjugating mirror, where the spectral lineshape of the Rb transition at 780 nm is roughly equivalent to a finite response time between 100–300 ps, i.e., well within the range studied here. The main result reported in the above-mentioned reference is a stability diagram indicating the various types of experimentally observed behavior as a map in the feedback level versus detuning plane. A narrow locking range extending into the negative detunings was observed, as well as the Hopf-bifurcation instability boundary, in agreement with our theory. The predicted return to stable locking for high feedback levels could not be observed in the experiment, simply because the spectral filtering of the feedback light did not allow the necessary high feedback strengths.

IV. Noise Spectra

In order to determine the optical spectra, we Fourier transform the linearized rate-equations. This yields

$$\tilde{\mathbf{x}}(\omega) = (i\omega I - A - e^{-i\omega\tau}A')^{-1}\tilde{\mathbf{F}}(\omega). \tag{15}$$

Here, $\tilde{\mathbf{x}}(\omega)$ is the Fourier transform of $\mathbf{x}(t)$, and $\tilde{\mathbf{F}}(\omega)$ that of the vector $\mathbf{F}(t)$ containing the Langevin noise. From (15), one finds how spontaneous emission affects the power and phase

$$\delta\tilde{P}(\omega) = \frac{1}{\Delta(\omega)}[M_{11}(i\omega)\tilde{F}_p(\omega) - M_{21}(i\omega)\tilde{F}_\phi(\omega)] \tag{16}$$

$$\delta\tilde{\phi}(\omega) = \frac{1}{\Delta(\omega)}[-M_{12}(i\omega)\tilde{F}_p(\omega) + M_{22}(i\omega)\tilde{F}_\phi(\omega)] \tag{17}$$

where $\Delta(\omega)$ is the determinant of $i\omega I - A - e^{-i\omega\tau}A'$. In terms of the determinant, $D(s)$ found by Laplace transformation in the stability analysis of a laser with PCF (see Section III), $\Delta(\omega)$ is equal to $D(i\omega)$. Furthermore, $M_{ij}(i\omega)$ are the minors of $i\omega I - A - e^{-i\omega\tau}A'$. The noise forces have correlation functions given by $\langle F_p(t)F_p(t')\rangle = 2RP\delta(t-t')$, $\langle F_p(t)F_\phi(t')\rangle = 0$, and $\langle F_\phi(t)F_\phi(t')\rangle = R/2P\cdot\delta(t-t')$, and we arrive at the following

equations for the relative intensity noise (RIN) and frequency noise spectrum (FNS) in the steady state:

$$S_{\mathrm{RIN}}(\omega) = \frac{R}{|\Delta|^2\sqrt{2\pi}}\left(\left|M_{11}^2\right|\frac{2}{P_s} + |M_{21}|^2\frac{1}{2P_s^3}\right) \quad (18)$$

$$S_{\dot{\phi}}(\omega) = \frac{\omega^2}{|\Delta|^2\sqrt{2\pi}}\left(|M_{12}|^2 2RP_s + |M_{22}|^2\frac{R}{2P_s}\right) \quad (19)$$

A. Results

Using the expressions derived in the previous section, we calculate the RIN and FNS for the case of zero pump-detuning ($\delta_0 = 0$). We take the the laser to be pumped 50% above threshold, $J = 5.805\cdot 10^{17}$ s^{-1}. We do this because 50% above threshold the intensity fluctuations due to spontaneous emission are much smaller than at 5% above threshold. Therefore, we expect the linearized rate equations to give a better description. Furthermore, we assume linear gain ($\epsilon = 0$). The other parameters are taken from Table I. With these parameter values, the RO frequency ω_R of the solitary laser is 2.415 GHz. The relevant stability diagrams for these parameters are sketched in Fig. 3. In the first instance, we investigate the low-feedback stable region, assuming a feedback rate $\gamma_p = 10\cdot 10^7$ s^{-1}, and consider the high-feedback steady state later on.

In Figs. 4 and 5(a), the RIN and frequency noise spectra are depicted for an instantaneous mirror and a PCM with a 400-ps response time. The delay time in the external cavity is 207 ps, which implies a steady state 'under the first peak' in Fig. 3(a). The spectra for the solitary laser are shown for comparison. The spectra agree qualitatively with those obtained by Agrawal and Gray [7] and Petersen *et al.* [20] for an instantaneous PCM. There is one clear discrepancy, however. Compared with the solitary laser, Agrawal and Gray see a shift of the RO frequency in the laser with PCF, whereas Petersen and we do not see such a shift. We think this difference is due to the fact that [7] has approximated the exponential $e^{i\omega\tau}$ by $1+i\omega\tau$, which we argued can be problematic (see Section III). Note that the frequency noise approaches zero when $\omega \to 0$. This is due to the phase-compensating nature of a PCM, which fixes the phase in the long run. The figures also show a slight enhancement of the RO peak for the PCM with 400-ps response time. We address this point later on. In the sequel, we consider only the calculation of the FNS. We do this because, apart from the gross features seen in the figures, the FNS and RIN spectrum show similar behavior; for example, a resonance in the FNS is generally seen in the RIN spectrum as well. Furthermore, the most important effect of phase-conjugate feedback is on the *phase*.

The FNS when the mirror is placed twice as far from the laser ($\tau = 404$ ps, $\omega_R\tau/2\pi = 1$) is plotted in Fig. 5(b). This spectrum is almost identical to the spectrum in Fig. 5(a), except for a substantial rise in the RO peak for an instantaneous mirror. Calculation of several more noise spectra shows that, for $t_m = 0$, the height of the RO peak changes periodically with the cavity length; it is highest when $\omega_R\tau/2\pi$ is an integer, and lowest when $\omega_R\tau/2\pi$ is a half-integer. The reason for this is clearly the same as the origin of the modulation in the stability diagram Fig. 3: when the RO matches an external round-trip resonance, the stability is decreased.

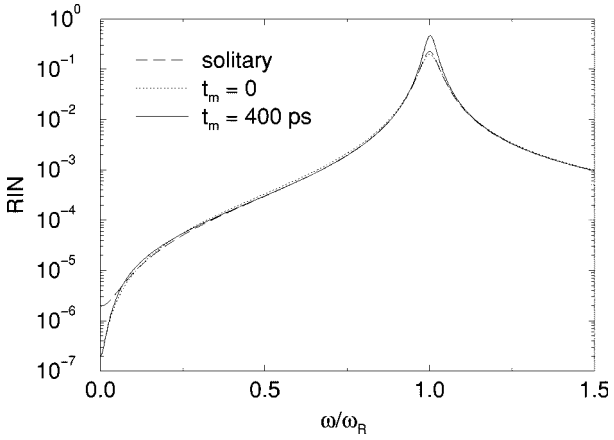

Fig. 4. RIN spectrum in the low feedback regime. The external delay time is 207 ps, corresponding to $\omega_R\tau/2\pi = 0.5$.

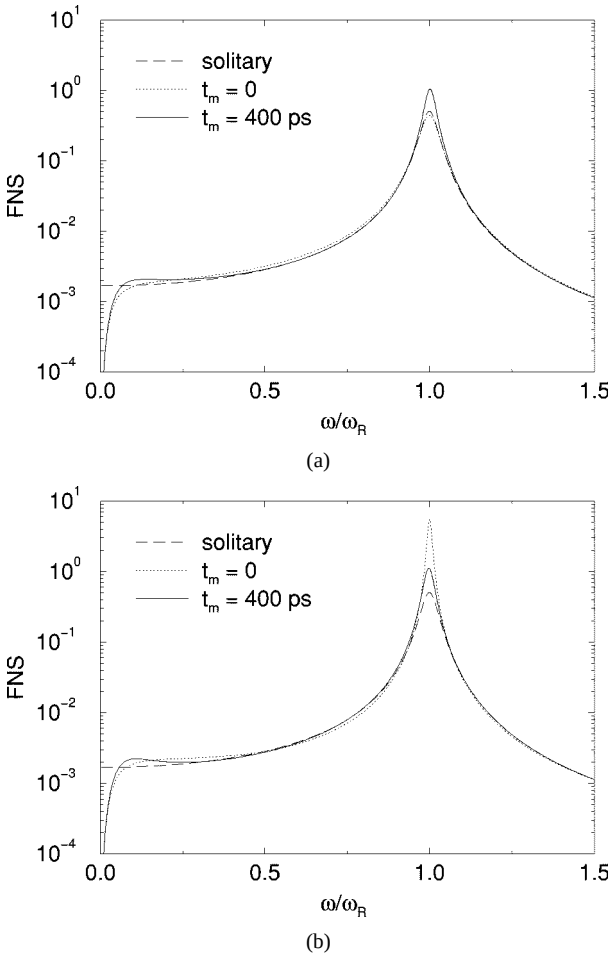

Fig. 5. The frequency noise spectrum in the low feedback regime. (a) The external delay time is such that $\omega_R\tau/2\pi = 0.5$. (b) $\omega_R\tau/2\pi = 1$.

The variation of the height of the RO peak with the cavity length is not seen when the PCM has a 400-ps response time. We explain this by the fact that, for large t_m, the mirror tends to diffuse the quality of the resonance because the cavity length is not so sharply defined anymore [see Fig. 1(a) and the discussion there, and Fig. 3(a)]. Therefore, for large t_m, the round-trip resonances are less well-defined. This phenomenon shows up when t_m becomes of the order of the RO period (=414 ps). This is

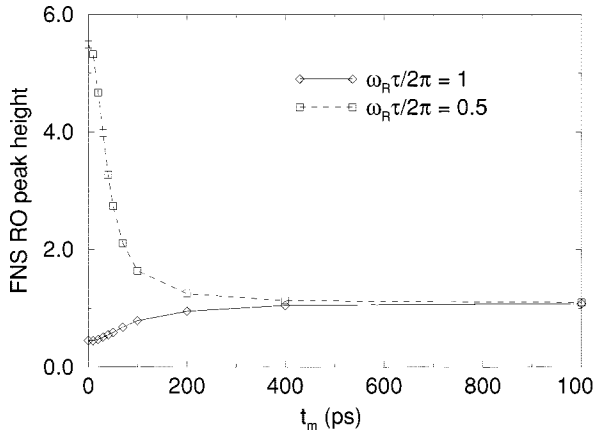

Fig. 6. The height of the RO peak as a function of the mirror response time t_m. The external delay times are 207 ps (dashed curve, $\omega_R\tau/2\pi = 0.5$) and 414 ps (solid curve, $\omega_R\tau/2\pi = 1$); see also Fig. 3.

seen clearly in Fig. 6, where we have plotted the height of the RO peak as a function of the mirror response time for external delay times τ =207 ps (where the peak is relatively minimum) and τ =414 ps (where the peak is relatively maximum). For mirror response times larger than about 200 ps, the height of the RO peak in the FNS is almost insensitive to the external cavity length.

We now come to the spectra of the laser in the upper stability regime (see Fig. 3(b) for the relevant stability diagram). Because the laser with PCF from an *instantaneous* mirror does not become stable for higher feedback-levels, we must consider finite response times ($t_m \gtrsim 100$ ps). The frequency noise spectra for a solitary laser and a laser with a 100- or 400-ps PCM are depicted in Fig. 7(a) for a feedback rate $\gamma_p = 4000 \cdot 10^7$ s^{-1} and a 10-cm external cavity (τ =667 ps). Especially for $t_m = 100$ ps, resonances are seen. Also, Petersen [20] and Bochove [14] found such oscillations in their spectra for an instantaneous mirror with $t_m = 0$. These resonances are not related to the RO, but correspond to the double-round-trip modes which were first described by AuYeung *et al.* [21]. Apart from the fact that the larger mirror response time almost washes out these resonances at t_m =400 ps, the spectra for 100 and 400 ps are equal. Comparison with the spectrum of the solitary laser shows that the RO peak has disappeared. A broad resonance at about 2.7 times the RO frequency is found instead. Furthermore, the overall noise level is decreased by several orders of magnitude.

In order to understand the origin of the peak at $\omega = 2.7\omega_R$, we consider a short cavity (L = 1 cm, τ = 66.7 ps) and a mirror response time of 400 ps. Because of the short cavity length, the double round-trip resonances do not obscure the peak under consideration so much, an effect which is enhanced by the relatively large value of t_m. With these parameters, the FNS is shown in Fig. 7(b) for several feedback rates, ranging from 3500 to 6000 $\cdot$ 10^7 s^{-1}. The frequency Ω of the main resonance increases with γ_p, whereas the total noise level is drastically reduced. It turns out that, in good approximation, Ω varies linearly with γ_p (the dependence is slightly superlinear), at least in the interval considered. The variation of several other laser parameters does not reveal any substantial influence on the frequency Ω.

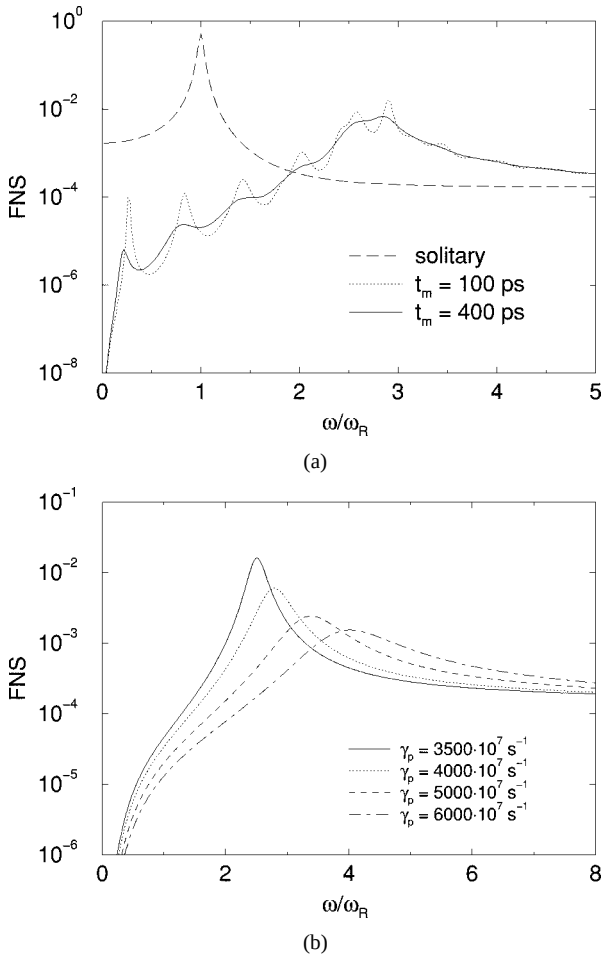

Fig. 7. (a) FNS for a solitary laser and for a PCF laser with parameters $\gamma_p = 4000 \cdot 10^7$ s^{-1} and τ =667 ps. (b) FNS for several feedback rates for t_m =400 and τ =66.7 ps.

A feeling for the origin of the resonance at Ω can be obtained by realizing that there is a frequency in the laser-with-PCF system that is proportional to the feedback strength: the laser resonance frequency at a given inversion N with respect to the solitary laser frequency is given by

$$\omega(N) = \frac{1}{2}\alpha\xi(N - N_{\rm th}), \tag{20}$$

while for zero pump-detuning, the inversion N depends linearly on γ_p [see (9)]. Combining (20) with (9) yields

$$\Omega = \frac{\alpha}{\sqrt{1+\alpha^2}}\gamma_p. \tag{21}$$

This explains why Ω does not depend on other parameters. Even the dependence on α is very limited since $\alpha/\sqrt{1+\alpha^2}$ is almost equal to one when $\alpha > 1$. Below, we analyze the roots of the characteristic equation $D(s) = 0$, and this yields the same result [(21)] when γ_p large.

Now we try to find the dependence of the frequency Ω found in the frequency noise spectra at high feedback-rates from the characteristic equation $D(s) = 0$ as given by (14). This is expected to yield relevant information since the expression (19) for the FNS is inversely proportional to $\Delta^2(\omega) = D^2(i\omega)$. In the spectra calculated in this section, we did not find a noticeable dependence of Ω on the cavity length up to cavities as short as 0.5 cm. This motivates us to consider the case of

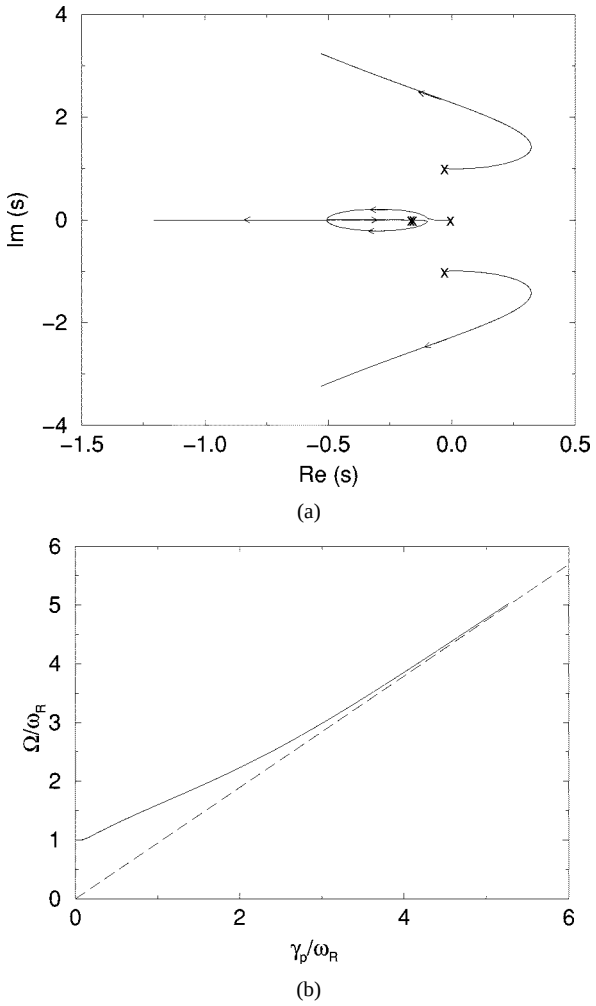

Fig. 8. (a) Eigenvalues of the characteristic equation for $\tau = 0$ move in the complex plane as a function of γ_p. The crosses indicate the locations at $\gamma_p = 0$. (b) The imaginary part of the eigenvalue corresponding to the RO at low feedback rate as a function of the feedback rate (solid curve). The dashed line gives the high-feedback-rate limit.

zero cavity-length $\tau = 0$ in approximating the roots. In doing so, $D(s)$ simplifies considerably, and it is easy to follow the roots of the resulting polynomial of degree five numerically as a function of γ_p. The roots move in the complex plane as indicated in Fig. 8(a). Three roots are found to move in the negative half-plane $(\mathrm{Re}(s) < 0)$, while the other two form a complex conjugate pair which crosses the imaginary axis twice. Focusing on the solution of this complex conjugate pair which has a positive imaginary part, it is found that is has a negative real part and an imaginary part equal to ω_R for $\gamma_p = 0$, corresponding to a damped RO. Upon increasing γ_p, it moves to the right and crosses the imaginary axis in a Hopf bifurcation, which is the undamping of the RO. Then it bends upward (the frequency starts increasing) and, finally, it moves back to the negative half-plane (the laser becomes stable again) while the frequency keeps increasing. We have plotted the imaginary part of the eigenvalue as a function of γ_p in the right of Fig. 8(b). For $\gamma_p = 4000 \cdot 10^7\ \mathrm{s}^{-1} = 2.6\omega_R$, the imaginary part of the eigenvalue is $2.6\omega_R$, in agreement with the $2.7\omega_R$ found from Fig. 7.

It is possible to find the relevant root of $D(s) = 0$ analytically for large feedback rates. We then assume γ_p to be larger than all other inverse time scales: the inverse mirror response time, the RO frequency, and the RO damping rate. The characteristic equation then simplifies to

$$s^5 + 2\gamma_p \cos\beta_s s^4 + \gamma_p^2 s^3 = 0. \tag{22}$$

With $\beta_s = -\arctan\alpha$ (which holds when $\delta_0 = 0$), the solutions are

$$s = 0 \quad \text{and} \quad s = \left(\frac{-1}{\sqrt{1+\alpha^2}} \pm i\frac{\alpha}{\sqrt{1+\alpha^2}}\right)\gamma_p. \tag{23}$$

For large values of γ_p, the frequency Ω therefore reads

$$\Omega = \frac{\alpha}{\sqrt{1+\alpha^2}}\gamma_p \tag{24}$$

in accordance with (21). Ω depends linearly on γ_p, and this has been plotted in Fig. 8(b) (dashed line). It can be seen that (21) yields a good description when $\gamma_p \gtrsim 3\omega_R$.

This resonance explains the frequency dependence of the pulsations of the laser with a 400-ps response time PCM as found by DeTienne *et al.* [11]. In a numerical simulation, they found that the frequency of the pulsations (with a modulation depth of 100%) depends almost linearly on the feedback rate. We have calculated the roots of the simplified (we have taken $\tau = 0$) characteristic equation using their parameters and found excellent agreement. Hence, the pulsating behavior of the laser in the unstable (nonmonochromatic light emission) regime and the resonance in the noise spectra in the stable regime have a common origin in the detuning between the eigenfrequency (20) of the compound system and the actual lasing frequency as posed by the mirror pump beams.

V. Conclusion

We have performed an exact linear-stability-analysis of a single-mode semiconductor laser with filtered phase-conjugate feedback from a mirror that is pumped externally. In the weak-feedback part of the (γ_p, τ)-plane, the periodic modulation of the stability-edge curve is due to the effective external delay time being an integer multiple of the relaxation oscillation period. A finite mirror-response time tends to stabilize the system: the low-feedback stability-edge curve shifts upwards with t_m. This can be understood physically from the filtering nature of the PCM. Upon further increase of the feedback rate, the PCF laser becomes stable once more if the mirror has a finite response time. This new stability region is in sharp contrast to the unstable behavior of a laser with an instantaneously responding mirror with the same amount of feedback. The stability areas for low and moderate feedback are not two distinct regimes, but they are connected in the $(\gamma_p, \tau, \delta_0)$-space, which is apparent from the (γ_p, δ_0)-slice shown in Fig. 2(a). This picture, in a sense, unifies the two figures of Fig. 1.

For a diode laser with phase-conjugate feedback, we have calculated noise spectra, where we focused on the frequency noise. The height of the RO resonance for a laser with instantaneous PCF is very sensitive to the external cavity length: when the RO period fits the external cavity an integral number of times, the height of the RO peak is enhanced. A finite mirror-response time larger than $2\pi/\omega_R$ effectively washes out this sensitive dependence on τ. In the high feedback regime (which is found for

finite t_m only), the frequency noise is reduced drastically. Also, the main resonance is found to increase almost linearly with the feedback rate and can easily obtain frequencies as high as $3\omega_R$. This resonance is attributed to the inversion dependence of the intrinsic laser resonance, where the inversion is changed due to the feedback. This situatioin is similar to the case of injection locking. It also explains the behavior of the pulsation frequency found in simulations by DeTienne *et al.* [11].

APPENDIX
PRINCIPLE OF THE ARGUMENT

The method we use for testing whether the characteristic equation $D(s) = 0$ has roots in the left half-plane (LHP) is very much related to the Nyquist Analysis in engineering sciences [22]. It has previously been applied[1] to a laser with conventional optical feedback by Jaskorzyńska and Lenstra [23] and Cohen *et al.* [10]. It is based on the following theorem from the theory of functions of one complex variable [22].

Theorem 1: If C is a closed contour in the complex s-plane and $f(s)$ is an analytic function on and inside C, except for a finite number of poles inside C, and $f(s) \neq 0$ on C, then

$$\frac{1}{2\pi i}\oint_C \frac{f'(s)}{f(s)}\,ds = Z - P \tag{25}$$

where

Z total number of zeros inside C;
P total number of poles inside C;
$f'(s)$ $= df(s)/ds$.

With the well-known expression for the winding number, one sees that

$$Z - P = \frac{1}{2\pi}[\arg f(s)]\Big|_C. \tag{26}$$

Since C is closed, the image of C in the $f(s)$-plane is closed, and the net change in the angle $\arg f(s)$ is 2π times the number of encirclements N of the origin in the $f(s)$-plane. The result that $Z - P = N$ is often called the *principle of the argument*.

We apply this theorem to the function $f(s)$ given by

$$f(s) = \frac{D(s)}{(s+1)^4} \tag{27}$$

and introduce the variable $u = f(s)$. We choose the contour C to be a semicircle in the right half-plane (RHP) and close it along the imaginary axis [see Fig. 9(a)]. In the limit $R \to \infty$, the contour C encloses the entire RHP. The image of C under f in the u-plane is called Γ. Clearly, $f(s)$ does not have any poles in the RHP. Since the laser is stable if and only if the zeros of $f(s)$ are in the LHP, the criterion for stability is that the image Γ of C does not enclose the origin (the total number of encirclements N is zero). It is easily verified that $f(s^*) = f^*(s)$, and because C is symmetric in the real axis, Γ is too. Denoting the arc connecting the points a, b, and c by $\overline{abc}$, we only consider the image $\overline{a'b'c'}$ of the upper part $\overline{abc}$ of the contour C. The image of the lower part $\overline{cda}$ is found by reflection in the real axis (see Fig. 9).

[1]Notice that DiStefano *et al.* [22] define a *clockwise* traverse around a contour as the *positive* direction, and all points to the *right* of a contour when it is traversed in a prescribed direction as being *enclosed* by it. This is different from most mathematical literature.

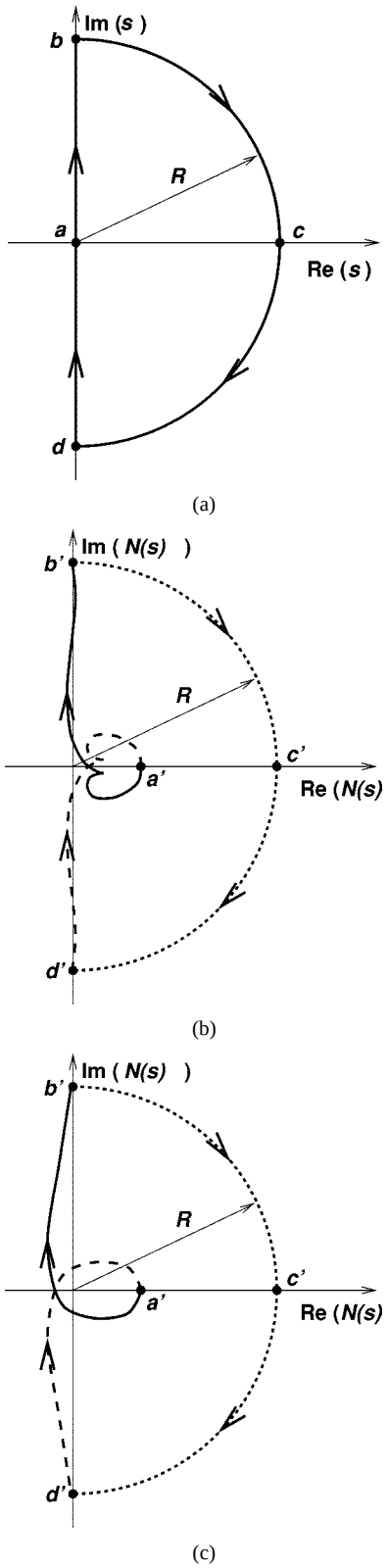

Fig. 9. (a) The contour C (in the s-plane) encloses the entire RHP in the limit $R \to \infty$. The other two figures are sample contours in the Γ-plane. (b) The origin is not enclosed and the laser is therefore stable. (c) The laser is unstable since the contour Γ encloses the origin.

Since for R very large, one has $f(s = \mathrm{Re}^{i\phi}) \approx \mathrm{Re}^{i\phi}$, the segment $\overline{bc}$ maps onto almost the same segment in the u-plane. The image $\overline{a'b'}$ of the remaining segment $\overline{ab}$ must now be such that

the total image contour Γ does *not* enclose the origin. In a situation where $\overline{ab}$ maps as sketched in Fig. 9(b), the laser is stable, whereas Fig. 9(c) represents an unstable situation.

It is seen that when $f(0)$ (which is a real number) is negative, the origin is encircled by Γ and the laser is unstable. This corresponds to the case $D(0) < 0$ in Section III.

The number of encirclements can be found by counting the number of intersections of $\overline{a'b'}$ with the negative real axis. If $\overline{a'b'}$ crosses this half-line as many times going up as going down, the number of encirclements is zero and hence the laser is stable. We have determined the number of intersections numerically.

Appendix
Coefficients

First we write the Laplace transform of the linearized rate equations as

$$(sI - A - C)\tilde{\mathbf{x}}(s) = \mathbf{x}(0) \tag{28}$$

where A is the part with $\epsilon = \beta = 0$. The matrix C represents the contribution of noise and nonlinear gain. From this we derive the inverse transfer matrix $sI - A - C$ with (for noninstantaneous PCF)

$$A = \begin{pmatrix} a_{11} & a_{12} & a_{13} & -a_{11} & a_{12} \\ a_{21} & a_{11} & a_{23} & -a_{21} & a_{11} \\ a_{31} & 0 & a_{33} & 0 & 0 \\ -a_{44}e^{-s\tau} & 0 & 0 & a_{44} & 0 \\ 0 & -a_{44}e^{-s\tau} & 0 & 0 & a_{44} \end{pmatrix} \tag{29}$$

and

$$C = \begin{pmatrix} c_{11} & 0 & c_{13} & 0 & 0 \\ 0 & 0 & 0 & 0 & 0 \\ c_{31} & 0 & c_{33} & 0 & 0 \\ 0 & 0 & 0 & 0 & 0 \\ 0 & 0 & 0 & 0 & 0 \end{pmatrix}. \tag{30}$$

For instantaneous PCF, the matrices A and C are given by

$$A = \begin{pmatrix} a_{11}(1 - e^{-s\tau}) & a_{12}(1 + e^{-s\tau}) & a_{13} \\ a_{21}(1 - e^{-s\tau}) & a_{11}(1 + e^{-s\tau}) & a_{23} \\ a_{31} & 0 & a_{33} \end{pmatrix} \tag{31}$$

and

$$C = \begin{pmatrix} c_{11} & 0 & c_{13} \\ 0 & 0 & 0 \\ c_{31} & 0 & c_{33} \end{pmatrix}. \tag{32}$$

The coefficients a_{ij} and c_{ij} are given by

$$a_{11} = -\gamma_p \cos\beta_s \tag{33}$$
$$a_{21} = \frac{\gamma_p}{2P_s} \sin\beta_s \tag{34}$$
$$a_{31} = -[\Gamma_0 + \xi(N_s - N_{\text{th}})] \tag{35}$$
$$a_{12} = -2\gamma_p P_s \sin\beta_s \tag{36}$$
$$a_{13} = \xi P_s \tag{37}$$
$$a_{23} = \frac{1}{2}\alpha\xi \tag{38}$$
$$a_{33} = -\left(\frac{1}{T_1} + \xi P_s\right) \tag{39}$$
$$a_{44} = -\frac{1}{t_m} \tag{40}$$
$$c_{11} = -\frac{4\beta N_s}{P_s} - \epsilon P_s \frac{G(N_s, P_s)}{1 + \epsilon P_s} \tag{41}$$
$$c_{31} = \epsilon P_s \frac{(2 + \epsilon P_s)[\Gamma_0 + \xi(N_s - N_{\text{th}})]}{(1 + \epsilon P_s)^2} \tag{42}$$
$$c_{13} = 4\beta - \epsilon P_s \frac{\xi P_s}{1 + \epsilon P_s} \tag{43}$$
$$c_{33} = \epsilon P_s \frac{\xi P_s}{1 + \epsilon P_s}. \tag{44}$$

The system determinant $D(s) = \det(sI - A - C)$ can, for finite response times, be written as

$$\begin{aligned} D(s) = {} & s^5 + d_4 s^4 + d_3 s^3 + [d_{20} + d_{21}\exp(-s\tau)]s^2 \\ & + [d_{10} + d_{11}\exp(-s\tau) + d_{12}\exp(-2s\tau)]s \\ & + [d_{00} + d_{01}\exp(-s\tau) + d_{02}\exp(-2s\tau)] \end{aligned} \tag{45}$$

where the coefficients d_{ij} are given by

$$d_4 = -\Gamma_{33} - C' + \frac{2}{t_m} \tag{46}$$
$$d_3 = -\Gamma_{13}\Gamma_{31} + \Gamma_{33}\left(C' - \frac{2}{t_m}\right) + \frac{1}{t_m^2} - \frac{2C'}{t_m} + B \tag{47}$$
$$\begin{aligned} d_{20} = {} & -\frac{1}{t_m}\left[\Gamma_{13}\Gamma_{31}(2 + A't_m) + \Gamma_{33}\left(Bt_m - 2C' + \frac{1}{t_m}\right)\right. \\ & \left. - 2B + \frac{C}{t_m}\right] \end{aligned} \tag{48}$$
$$d_{21} = \frac{D}{t_m} \tag{49}$$
$$d_{10} = -\frac{1}{t_m^2}[\Gamma_{13}\Gamma_{31}(1 + 2A't_m) - B + \Gamma_{33}(2Bt_m - C')] \tag{50}$$
$$d_{11} = -\frac{1}{t_m}\left(\Gamma_{13}\Gamma_{31}A' + \Gamma_{33}D - \frac{D}{t_m}\right) \tag{51}$$
$$d_{12} = -\frac{\gamma_p^2}{t_m^2} \tag{52}$$
$$d_{00} = -\frac{1}{t_m^2}(\Gamma_{13}\Gamma_{31}A' + \Gamma_{33}B) \tag{53}$$
$$d_{01} = -\frac{1}{t_m^2}(\Gamma_{13}\Gamma_{31}A' + \Gamma_{33}D) \tag{54}$$
$$d_{02} = \frac{\Gamma_{33}\gamma_p^2}{t_m^2}. \tag{55}$$

In order to facilitate the above expressions we introduced the parameters $A', B, C, D, \Gamma_{11}, \Gamma_{13}, \Gamma_{31}$, and Γ_{33}:

$$\Gamma_{13} = a_{13} + c_{13} \tag{56}$$
$$\Gamma_{31} = a_{31} + c_{31} \tag{57}$$
$$\Gamma_{33} = a_{33} + c_{33} \tag{58}$$
$$\Gamma_{13}A' = a_{12}a_{23} - a_{11}\Gamma_{13} \tag{59}$$
$$B = a_{11}c_{11} + \gamma_p^2 \tag{60}$$
$$C' = 2a_{11} + c_{11} \tag{61}$$
$$D = a_{11}c_{11}. \tag{62}$$

The system determinant for a laser with instantaneous feedback is obtained from (31) and (32). The resulting *third-order polynominal* can be found from (45) by multiplication with t_m^2 and taking the limit $t_m \to 0$.

For the calculation of the noise spectra, we need the minors $M_{11}(s), M_{12}(s), M_{21}(s),$, and $M_{22}(s)$. We express the minor $M_{ij}(s)$ as

$$M_{ij}(s) = m_{ij,4}s^4 + m_{ij,3}s^3 + [m_{ij,20} + m_{ij,21}\exp(-s\tau)]s^2 + [m_{ij,10} + m_{ij,11}\exp(-s\tau)]s + [m_{ij,00} + m_{ij,01}\exp(-s\tau)]. \quad (63)$$

The coefficients (for noninstantaneous PCF) are given by

$$m_{11,4} = 1 \quad (64)$$
$$m_{11,3} = \frac{2}{t_m} - H \quad (65)$$
$$m_{11,20} = I - \frac{2H}{t_m} + \frac{1}{t_m^2} \quad (66)$$
$$m_{11,21} = -\frac{a_{11}}{t_m} \quad (67)$$
$$m_{11,10} = \frac{1}{t_m}\left(2I - \frac{H}{t_m}\right) \quad (68)$$
$$m_{11,11} = \frac{a_{11}}{t_m}\left(\Gamma_{33} - \frac{1}{t_m}\right) \quad (69)$$
$$m_{11,00} = \frac{I}{t_m^2} \quad (70)$$
$$m_{11,01} = \frac{I}{t_m^2}, \quad (71)$$
$$m_{12,4} = 0 \quad (72)$$
$$m_{12,3} = -a_{21} \quad (73)$$
$$m_{12,20} = -\frac{2a_{21}}{t_m} - E \quad (74)$$
$$m_{12,21} = \frac{a_{21}}{t_m} \quad (75)$$
$$m_{12,10} = -\frac{2E}{t_m} - \frac{a_{21}}{t_m^2} \quad (76)$$
$$m_{12,11} = a_{21}\left(\frac{1}{t_m^2} - \frac{\Gamma_{33}}{t_m}\right) \quad (77)$$
$$m_{12,00} = -\frac{E}{t_m^2} \quad (78)$$
$$m_{12,01} = -\frac{a_{21}\Gamma_{33}}{t_m^2}, \quad (79)$$
$$m_{21,4} = 0 \quad (80)$$
$$m_{21,3} = -a_{12} \quad (81)$$
$$m_{21,20} = a_{12}\left(\Gamma_{33} - \frac{2}{t_m}\right) \quad (82)$$
$$m_{21,21} = -\frac{a_{12}}{t_m} \quad (83)$$
$$m_{21,10} = -a_{12}\left(\frac{1}{t_m^2} - \frac{2\Gamma_{33}}{t_m}\right) \quad (84)$$
$$m_{21,11} = \frac{a_{21}}{t_m}\left(\Gamma_{33} - \frac{1}{t_m}\right) \quad (85)$$
$$m_{21,00} = \frac{J}{t_m^2} \quad (86)$$
$$m_{21,01} = \frac{J}{t_m^2}, \quad (87)$$
$$m_{22,4} = 1 \quad (88)$$
$$m_{22,3} = \frac{2}{t_m} - G \quad (89)$$
$$m_{22,20} = F - \frac{2G}{t_m} + \frac{1}{t_m^2} \quad (90)$$
$$m_{22,21} = \frac{a_{11}}{t_m} \quad (91)$$
$$m_{22,10} = \frac{1}{t_m}\left(2F - \frac{G}{t_m}\right) \quad (92)$$
$$m_{22,11} = \frac{1}{t_m}\left(-I + \frac{a_{11}}{t_m}\right) \quad (93)$$
$$m_{22,00} = \frac{F}{t_m^2} \quad (94)$$
$$m_{22,01} = -\frac{I}{t_m^2}. \quad (95)$$

The following additional parameters were introduced for notational convenience:

$$\Gamma_{11} = a_{11} + c_{11} \quad (96)$$
$$E = a_{23}\Gamma_{31} - a_{21}\Gamma_{33} \quad (97)$$
$$F = \Gamma_{11}\Gamma_{33} - \Gamma_{13}\Gamma_{31} \quad (98)$$
$$G = \Gamma_{11} + \Gamma_{33} \quad (99)$$
$$H = a_{11} + \Gamma_{33} \quad (100)$$
$$I = a_{11}\Gamma_{33} \quad (101)$$
$$J = a_{12}\Gamma_{33}. \quad (102)$$

The minors obtained with instantaneous PCF are again obtained by multiplication with t_m^2 and taking the limit $t_m \to 0$.

REFERENCES

[1] M. W. Fleming and A. Mooradian, "Fundamental line broadening of single-mode (GaAl)As diode lasers," *Appl. Phys. Lett.*, vol. 38, no. 7, pp. 511–513, Apr. 1981.

[2] G. H. M. van Tartwijk and D. Lenstra, "Semiconductor lasers with optical injection and feedback," *Quantum Semiclass. Opt.*, vol. 7, pp. 87–143, 1995.

[3] W. A. van der Graaf, "Nonlinear Dynamics of Semiconductor Lasers Driven by External Optical Fields," Ph.D. dissertation, Vrije Universiteit Amsterdam, Amsterdam, The Netherlands, Dec. 1997.

[4] B. Tromborg, J. H. Osmundsen, and H. Olesen, "Stability analysis for a semiconductor laser in an external cavity," *IEEE J. Quantum Electron.*, vol. QE-20, pp. 1023–1032, Sept. 1984.

[5] A. Yariv, "Phase conjugate optics and real-time holography," *IEEE J. Quantum Electron.*, vol. QE-14, pp. 650–660, Sept. 1978.

[6] G. H. M. van Tartwijk, H. J. C. van der Linden, and D. Lenstra, "Theory of a diode laser with phase-conjugate feedback," *Opt. Lett.*, vol. 17, no. 22, pp. 1590–1592, Nov. 1992.

[7] G. P. Agrawal and G. R. Gray, "Effect of phase-conjugate feedback on the noise characteristics of semiconductor lasers," *Phys. Rev. A*, vol. 46, no. 9, pp. 5890–5898, Nov. 1992.

[8] G. R. Gray, D. Huang, and G. P. Agrawal, "Chaotic dynamics of semiconductor lasers with phase-conjugate feedback," *Phys. Rev. A*, vol. 49, no. 3, pp. 2096–2105, Mar. 1994.

[9] A. Ritter and H. Haug, "Theory of laser diodes with weak optical feedback. I. Small signal analysis and side-mode spectra," *J. Opt. Soc. Am. B*, vol. 10, no. 1, pp. 130–144, Jan. 1993.

[10] J. S. Cohen, R. R. Drenten, and B. H. Verbeek, "The effect of optical feedback on the relaxation oscillation in semiconductor lasers," *IEEE J. Quantum Electron.*, vol. 24, pp. 1989–1995, Oct. 1988.

[11] D. H. DeTienne, G. R. Gray, G. P. Agrawal, and D. Lenstra, "Semiconductor laser dynamics for feedback from a finite-penetration-depth phase-conjugate mirror," *IEEE J. Quantum Electron.*, vol. 33, pp. 838–844, May 1997.

[12] M. Lax, "Classical noise IV: Langevin methods," *Rev. Mod. Phys.*, vol. 38, no. 3, pp. 541–566, July 1966.

[13] J. J. DiStefano, A. R. Stubberud, and I. J. Williams, *Feedback and Control Systems*, ser. Schaum's Outline Series, Singapore: McGraw-Hill Book Co., 1967.

[14] E. Bochove, "Theory of a semiconductor laser with phase-conjugate optical feedback," *Phys. Rev. A*, vol. 55, no. 5, pp. 3891–3899, May 1997.
[15] J. Mørk, B. Tromborg, and J. Mark, "Chaos in semiconductor lasers with optical feedback: Theory and experiment," *IEEE J. Quantum Electron.*, vol. 28, pp. 93–108, Jan. 1992.
[16] A. Murakami and J. Ohtsubo, "Dynamics and linear stability analysis in semiconductor lasers with phase-conjugate feedback," *IEEE J. Quantum Electron.*, vol. 34, pp. 1979–1986, Oct. 1998.
[17] M. Yousefi and D. Lenstra, "Dynamical behavior of a semiconductor laser with filtered external optical feedback," *IEEE J. Quantum Electron.*, vol. 35, pp. 970–967, June 1999.
[18] A. Gavrielides, V. Kovanis, and T. Erneux, "Analytical stability boundaries for a semiconductor laser subject to optical injection," *Opt. Commun.*, vol. 136, no. 3–4, pp. 253–256, Mar. 1997.
[19] O. K. Andersen, A. P. A. Fischer, I. C. Lane, E. Louvergneaux, S. Stolte, and D. Lenstra, "Experimental stability diagram of a diode laser subject to weak phase-conjugate feedback from a rubidium vapor cell," *IEEE J. Quantum Electron.*, vol. 35, pp. 577–582, Apr. 1999.
[20] L. Petersen, U. Gliese, and T. N. Nielsen, "Phase noise reduction by self-phase locking in semiconductor lasers using phase conjugate feedback," *IEEE J. Quantum Electron.*, vol. 30, pp. 2526–2533, Nov. 1994.
[21] J. AuYeung, D. Fekete, D. M. Pepper, and A. Yariv, "A theoretical and experimental investigation of the modes of optical resonators with phase-conjugate mirrors," *IEEE J. Quantum Electron.*, vol. QE-15, pp. 1180–1188, Oct. 1979.
[22] J. J. DiStefano, A. R. Stubberud, and I. J. Williams, *Feedback and Control Systems*, ser. Schaum's Outline, Singapore: McGraw-Hill, 1967, pp. 187–223.
[23] B. Jaskorzyńska and D. Lenstra, "Principle of the argument in stability analysis: Application to a single-mode laser with optical feedback," Dept. of Elect. Eng., Delft Univ. Technol.,, Delft, The Netherlands, Tech. Rep. 1983-16, Oct. 1983.

Wim A. van der Graaf was born in Eindhoven, The Netherlands in 1966. He received the M.Sc. degree in physical engineering from the Eindhoven University of Technology, and the Ph.D. degree from the Vrije Universiteit, Amsterdam. His dissertation work concerned the dynamics of semiconductor lasers driven by external optical fields.

Presently, he is a Quantitative Analyst with Fortis Bank, Central Risk Management, Amsterdam, The Netherlands. He is involved in the application of models to estimate the market risk, i.e., the possible change in value of a financial asset or portfolio due to the movement of market prices, often involving portfolios containing exotic derivative instruments.

Luis Pesquera, photograph and biography not available at the time of publication.

Daan Lenstra (M'97), photograph and biography not available at the time of publication.